White-Dwarfs in the thin-disk: physical properties and luminosity functions

Hektor Monteiro
Doutor em Astronomia
Pesquisador do Núcleo de Astrofísica Teórica (UNICSUL)
São Paulo – SP [Brasil]
hektor.monteiro@gmail.com

Wei-Chun Jao
Doutor em Astronomia
Pesquisador (Georgia State University)
Atlanta – GA [USA]
jao@chara.gsu.edu

Antonio Kanaan
Doutor em Física
Pesquisador (UFSC)
Florianópolis – SC [Brasil]
kanaan@if.ufrgs.br

In this article, we present an investigation of a sample of 1072 stars extracted from the *Villanova Catalog of Spectroscopically Identified White Dwarfs* (2005 on-line version), studying their distribution in the Galaxy, their physical properties and their luminosity functions. The distances and physical properties of the white dwarfs are determined through interpolation of their (B-V) or (b-y) colors in model grids. The solar position relative to the Galactic plane, luminosity function, as well as separate functions for each white dwarf spectral type are derived and discussed. We show that the binary fraction does not vary significantly as a function of distance from the Galactic disk out to 100 pc. We propose that the formation rates of DA and non-DAs have changed over time and/or that DAs evolve into non-DA types. The luminosity functions for DAs and DBs have peaks possibly related to a star burst event.

Key words: Binaries ages. Statistics. Stellar populations. White dwarfs.

1 Introduction

Stars with masses lower than 8 comprise the majority of objects in the Galaxy, and will eventually evolve into electron-degenerate white dwarfs (WDs), making them the most common end product of stellar evolution. WDs are essentially degenerate plasmas, governed by well understood physical processes, and are one of the most useful classes of objects in the Galaxy because they are well-behaved cosmochronometers – for a detailed discussion, see Fontaine et al. (2001). Consequently, WDs have been used to understand degenerate physical processes, stellar evolution, and Galactic formation and evolution.

White dwarfs have been commonly used as tracers of old Galactic populations. For example, in Sion et al. (1988), the authors analyzed a sample of stars from the McCook & Sion (1977) catalog. Based on published observational data and on the derived effective temperatures, radii, masses, and kinematics of hundreds of WDs of various spectral types, the authors found that there is no kinematic difference between DA and DB stars of similar color and magnitude, and that magnetic degenerate stars are a kinematically distinct group of young disk objects. Based on the general kinematic similarity of DA stars and their non-DA counterparts, the authors also inferred that neither evolved from more massive WD progenitors.

Because WDs cool predictably with age, they provide a means to estimate important timescales, such as the timing of early star formation events in the Galaxy. Luyten (1958), Sion and Liebert (1977), Greenstein (1979), and Sion et al. (1988) all estimated the WD local density and luminosity function. All efforts were successes to some extent, but were ultimately limited by statistically incomplete and small samples. Green (1980) constructed the WD luminosity function for a statistically complete sample, but was limited by small number of objects (89) and low quality spectra, which led to poorly estimated physical properties.

One of the luminosity function's most important features, the evident drop-off found at, was recognized not to be a simple effect of observational completeness but to be a consequence of the cooling processes in WDs. To put it simply, WDs have not had enough time to cool to fainter magnitudes. The possibility of linking this feature to the first burst of star formation has prompted researchers to attempt to use the luminosity function to obtain constraints for the age of the Galaxy (e.g. IBEN; LAUGHLIN, 1989; OSWALT et al., 1996; SALARIS et. al., 1997, and references therein). In Liebert et al. (1988), the authors presented arguably the benchmark study of the WD luminosity function. With careful attention to the sample used, as well as the most up-to-date models to determine WD physical properties, they estimated an age of 7 to 10 Gyr for the Galactic disk.

Based on the observational results of Liebert et al. (1988), Wood (1992) presented the first comprehensive theoretical study of the parameter space that defines the luminosity function, including more realistic treatments of cooling, star formation rates and bursts, as well as scale-height inflation. The author shows the luminosity function as particularly sensitive to star formation rates and bursts, as well as WD core composition. The author finds that the luminosity function is insensitive to the assumed initial mass function, scale height, and WD progenitor mass upper limit.

After these efforts, many others have followed with improved samples and variations in the theoretical procedure of obtaining a fit to an observed luminosity function. Wood & Oswalt (1998) present a good summary of these papers, as well as a very thorough discussion of uncertainties inherent to the commonly used method of obtaining the

observed luminosity function. However, two limitations hinder these studies: limited samples and poor distance determinations. These issues have been addressed by Harris et al. (2006), in which the authors determine a luminosity function for a large sample of WDs from the Sloan Digital Sky Survey, but they were limited by the lack of spectral types and robust distance estimates.

To address these issues, we revisit the *Villanova Catalog of Spectroscopically Identified White Dwarfs*, one of the largest and most comprehensive WD catalogs to date, in its latest version (November 2005) as available through *Vizier*. Based on up-to-date theoretical WD models, we obtain reliable distance estimates for a large set of objects in the catalog. We, then, investigate the spatial distribution of this sample in the Galaxy, their binary fraction and their physical properties. With a well-defined sample and robust distance estimation, we also construct the luminosity functions using the well-established method. Finally, we deconstruct the total luminosity function into its individual components based on the various WD spectral types as listed in the original catalog.

2 Estimating reliable distances

To perform a statistical study of stars, one needs a large sample of objects to which distances are known or can be estimated. In the *Villanova Catalog*, distances come from many sources and therefore are not uniformly determined. For the WDs with parallaxes, we adopted those distances with as correct. To avoid introducing unknown biases, we re-estimated the distances for WDs that did not have parallaxes. Table 1 shows the numbers of stars, also discriminated by spectral type, for which we adopted parallax or estimated distances.

Table 1: Spectral type numbers in sample used and distance adopted

		Estimated distance
Total	184	888
DA	115	730
DB	9	64
DC	36	59
DZ	7	15
DQ	17	20

Source: The authors.

The procedure used to estimate distances consisted of interpolating observed colors in existing model grids. We used the curves defined by [,(*B*-*V*)] or [,(*b*-*y*)] for WDs with a given *Log*(*g*) and composition. The observed colors of an object are then interpolated in these curves to obtain its absolute magnitude, which combined with the observed *V* magnitude, gives its distance. Monteiro et al. (2006) used this procedure to determine ages for two WD-subdwarf systems, and we have modified it to estimate distances.

We used the Bergeron et al. (1995) grid of models, assuming 1) *log*(*g*)= 8.0 and 2) DA or non-DA models (based on the catalog spectral classification) for the WDs in the sample. The narrow distribution of *Log*(*g*) values shown for DA and DB WDs with *log*(*g*)= 7.99 and *log*(*g*)= 8.22, respectively [see Bergeron et al. (2001) for details], justifies that assumption. First, we determined the procedure's accuracy, comparing the model estimated distances to distances determined from parallax measurements that were available. Figure 1 shows the comparison of parallax distances and model estimated distances. The average error between the estimated distance and the parallax distance for the set of objects is of 26%. We adopt this as the general accuracy for this method.

We, then, estimated the distances for objects in the *Villanova Catalog* that had *V* magnitude, (*B*-*V*) color or (*b*-*y*) color and for which no reliable parallax measurements were available. We adopt-

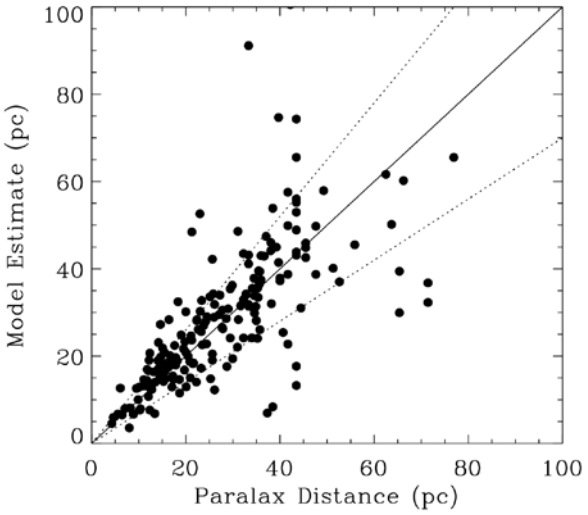

Figure 1: Comparison of the model estimated distances and parallax distances for WDs in the sample used in this work. Dotted lines indicate the 30% error boundary

Source: The authors.

ed the catalog's spectral classification of individual WDs to assign each WD to DA or non-DA model grid. Thus, stars were separated into DA and non-DA samples for the application of H or He model grids, respectively, as described in Bergeron et al. (2001). As shown in table 1, a total of 184 WDs and 888 WDs with estimated distances comprise the final sample.

3 Distribution of WDs in the galaxy

3.1 The binary fraction

One of our objectives in this work was to investigate how the properties of the objects in our sample relate to their positions in the Galaxy and more precisely, to their distances to the Galactic disk. Figure 2 shows the distribution of the sample in the sky, as well as the distances to the disk as a function of the Galactic longitude. The reasonably uniform distribution of objects in the sky and the decreasing gradient away from the disk are evident. Visual inspection of this figure shows that there is no significant difference between the specified distributions of DA (open circles) and non-DA (filled circles) stars.

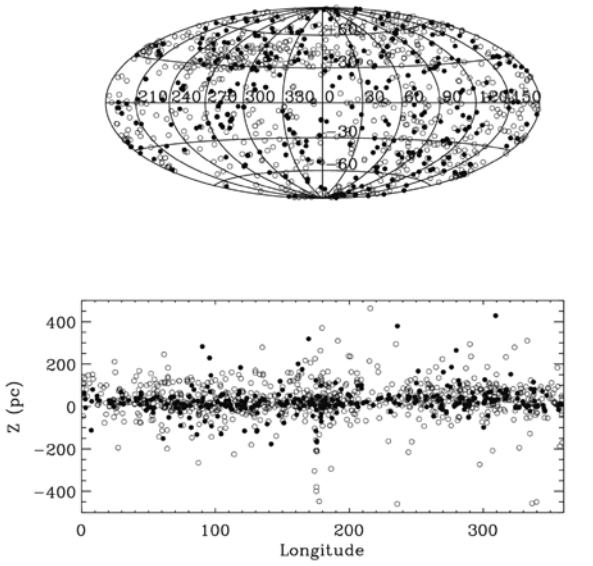

Figure 2: Distribution in the sky of the WD (DA open circles and Non-DA filled circles) sample of McCook (1999), 2003 version available through Visier. Top portion shows the Galactic projection and bottom part the "edge-on" view of the distribution

Source: The authors.

Our sample allows us to investigate whether any correlation exists between distance to the Galactic disk and binary fraction. To examine the potential correlation between disk distance z and binary fraction, we first corrected z for the solar offset. The correction was performed using the offset value determined by performing a Gaussian fit to the histogram of uncorrected z values and determining the offset of the Gaussian peak (Figure 3). In this fit we used Poisson weighting for the points, which gives higher importance for higher star counts, therefore leading to a poorer fit for the wings of the distribution. We found the solar distance to the disk to be above the plane defined by the WDs. This value is in general agreement

with the ones published by Humphreys & Larsen (1995), in which a thorough discussion of the solar distance to the plane is made. Using the corrected values, we plotted the number of single and binary WD systems (as defined in the *Villanova Catalog*) out to 100 pc in bins of 10 pc (Figure 4, upper left panel), and then divided the two distributions to obtain the binary fraction (Figure 4, upper right). In the lower panels of Figure 4, we show the results of applying the same procedure as before, but plotting counts as a function of distance to the Sun. In this procedure stars such as Sirius A and B were considered as one system to be consistent with the unresolved binaries in the sample.

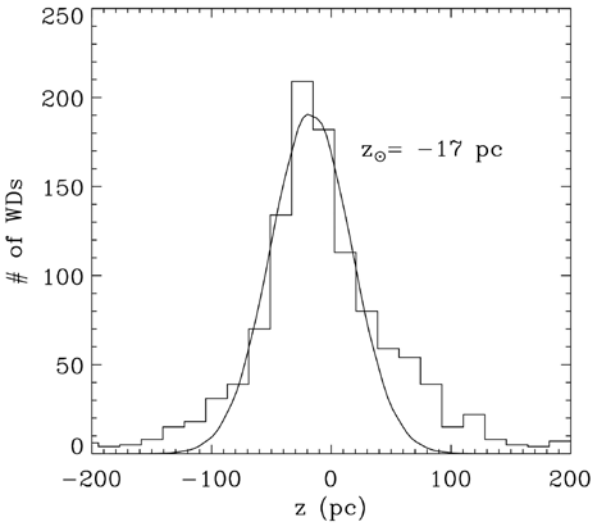

Figure 3: Determination of the solar distance to the Galactic disk. We constructed a histogram with the uncorrected z values for the WDs and then fit a Gaussian to the distribution. The offset of the Gaussian peak relative to the position z=0 was then adopted as the solar offset

Source: The authors.

The flat nature (within the errors) of the binary fraction (Figure 4, lower right panel) indicates that both single and binary WD systems have similar detection biases as a function of distance, when considering the volume limited to 100 pc. We limited the distance to the value of 100 pc due to detection biases that can be present at higher distances. In particular, we needed to ensure that the efficiency for the detection of objects is basically the same for single WDs as well as for the binary WDs, before investigating their relative behavior. This is clearly demonstrated by the histogram of counts as a function of solar distance for single and binary WDs and the binary fraction derived from them. If there were systematic differences in the detection efficiency for the two types of objects, a change in the slope of the binary fraction would be evident. Inspecting the histogram of the binary fraction of WDs as a function of distance to the disk z (Figure 4 upper right), a slope in the binary fraction is not detected, at least within the errors. It is clear that this technique can provide some interesting results, but much larger samples with reliable binary classification are still needed.

3.2 The physical properties

We also investigated the relationship between the physical properties of the WDs that had reliable parallaxes and their positions in the Galaxy, using the procedure developed in Monteiro et al. (2006), which combines the absolute magnitude with the $(B\text{-}V)$ color and model grids to determine the physical properties of the WDs. To determine the errors in our procedure, we compared results from our method to those of Bergeron et al.(2001), who modeled WD physical properties using precise trigonometric parallaxes. It is clear from the results shown in figure 5 that the $log(g)$, T_{eff}, and cooling age are reasonably well-determined, with average errors under 20%, approximately. However, mass is less well-determined, with about 30% average errors. The objects found outside of the 20% regions typically fall outside the model grids available, and therefore, are subject to large extrapolation errors.

We proceeded with the determination of $log(g)$, T_{eff}, mass and cooling age for our sample using the method discussed above. With these

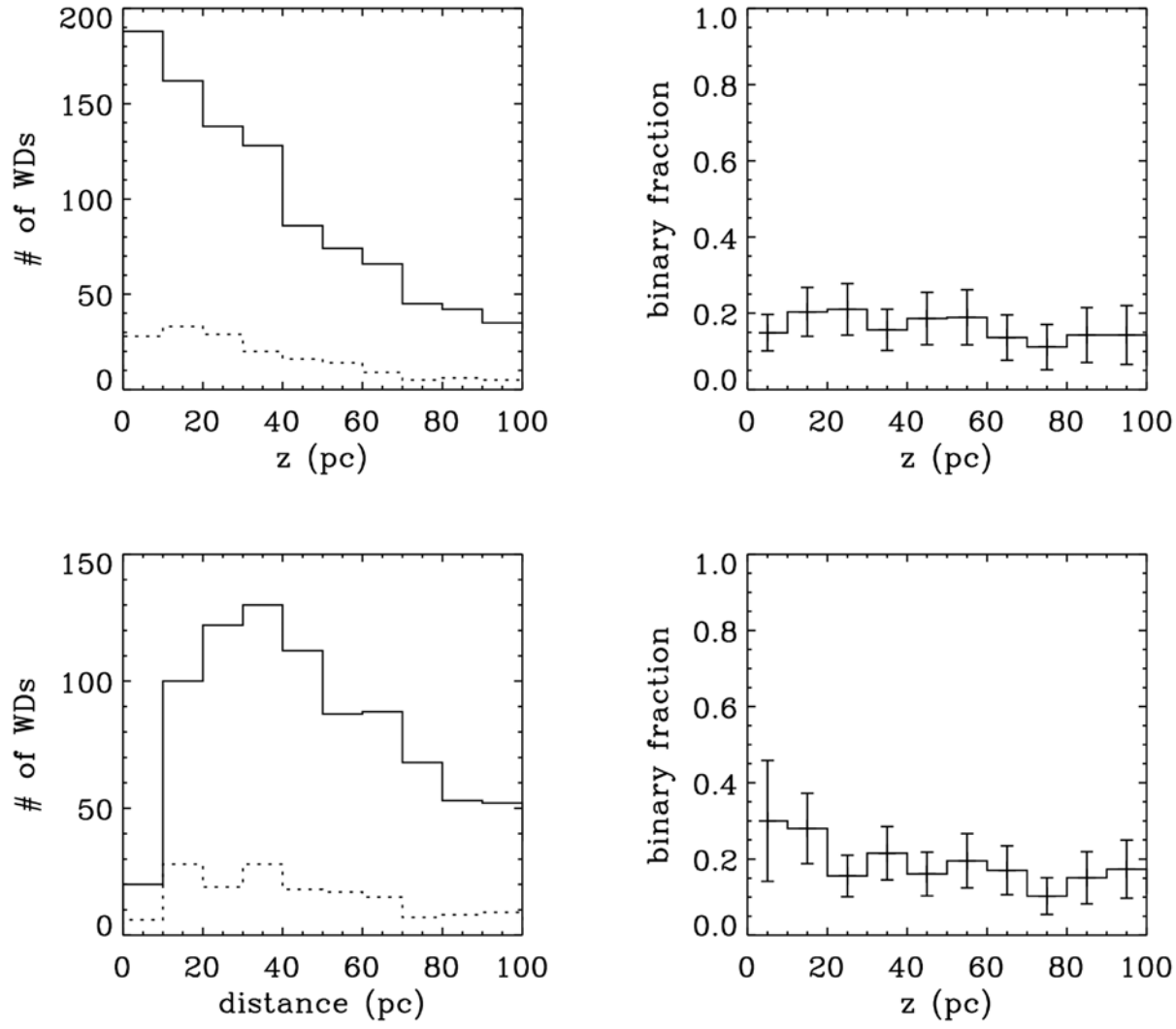

Figure 4: (Upper left) – Number of WDs as a function of the distance to the Galactic plane z (in parsecs) for single WDs (solid line) and binary WDs (dotted line). (Upper right) – Binary fraction as a function of the distance to the Galactic plane z (in parsecs). Error bars are given by simple Poisson counting uncertainty; (lower left) – Number of WDs as a function of the distance to the Sun (in parsecs) for single WDs (solid line), and binary WDs (dotted line); (Lower right) – Binary fraction as a function of the distance to the Sun (in parsecs) with the error bars given by simple Poisson counting uncertainty

Source: The authors.

physical characteristics determined, we constructed plots correlating each parameter to the distances of the WDs from the Galactic disk. The results are presented in Figure 6. There was no apparent correlation detected between the various physical characteristics and the distance to the Galactic disk *z*. It is clear, however, from these graphics that DA stars are on average hotter than non-DA and are, therefore, also younger (as can also be seen in the graphic for their cooling ages).

In Figure 7, we plot the histograms of the physical parameters for the sample, and in Figure 8, we plot the same histograms, discriminating between DA and non-DA WDs. The histograms for *log*(*g*) and mass in both figures show relatively narrow distributions and no significant differ-

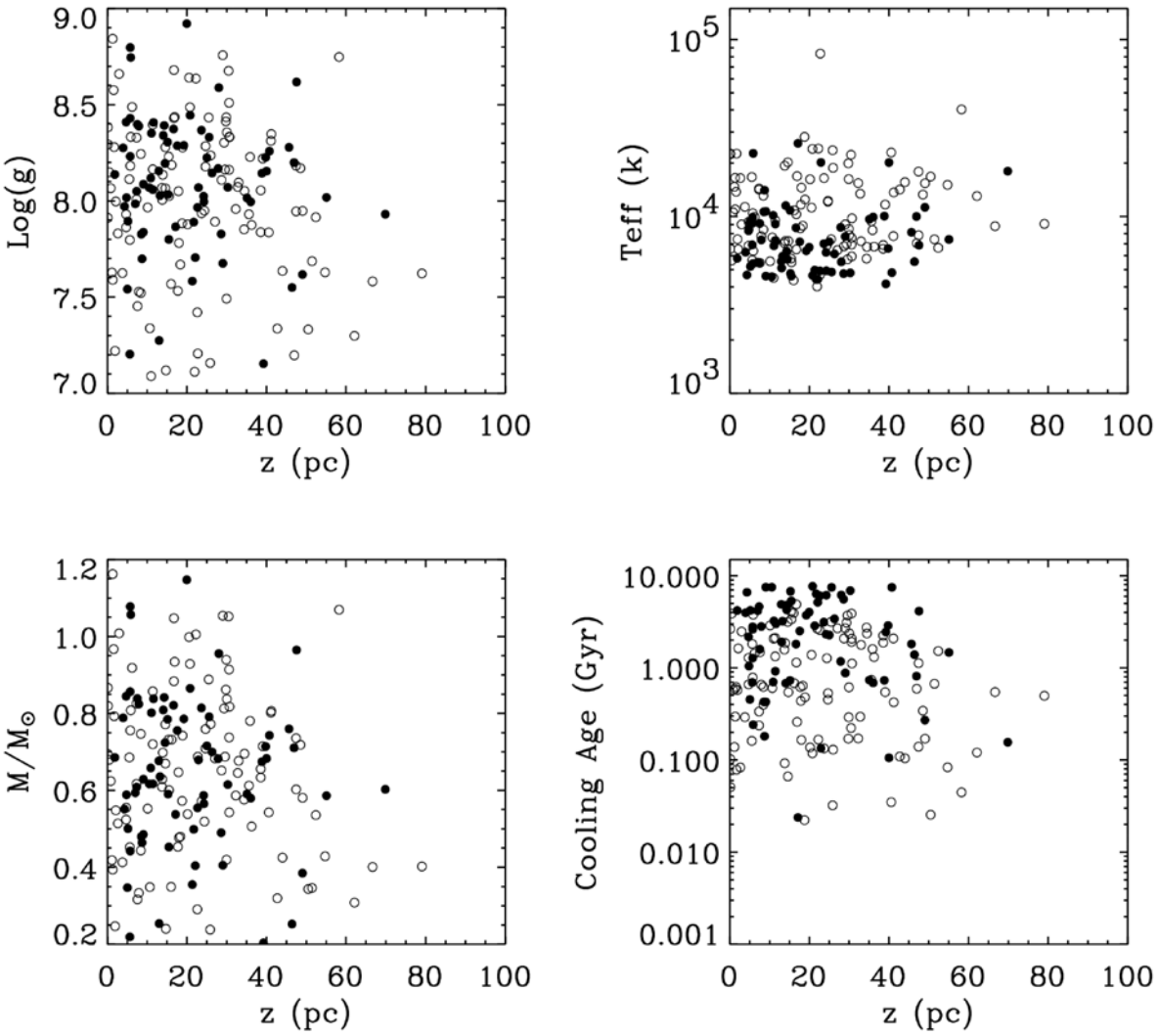

Figure 5: Comparison of our model interpolation results to those of Bergeron et al.(2001) with DA (open circles) and non-DA (filled circles). The dotted lines indicate the 20% difference regions

Source: The authors.

ences between DA and non-DAs. The histogram for $log(g)$, T_{eff}, with median around $log(g)$~8.1, is slightly skewed to higher values, likely due to contamination by unresolved binaries. The histograms for the cooling ages of DAs and non-DAs show that DAs are on average younger than non-DAs, and are not likely to be found with cooling ages greater than ~5 *Gyr*. On the other hand, we found cooling ages up to ~8 *Gyr* for non-DAs.

We also investigated the distribution of total ages for each WD spectral type. To accomplish this, we first adopted the initial to final mass relation (IFMR) of Weidemann (2000) to determine the progenitor masses for the WDs fitting the tabulated values using a third order polynomial:

$$M = 0.009 + (6.6M_{WD}) + (20.8M^{2}_{WD}) + (7.6M^{3}_{WD}) \quad (1)$$

in which M is the progenitor mass and M_{WD} is the mass of the white dwarf in solar masses. Finally, we used this polynomial in conjunction with the

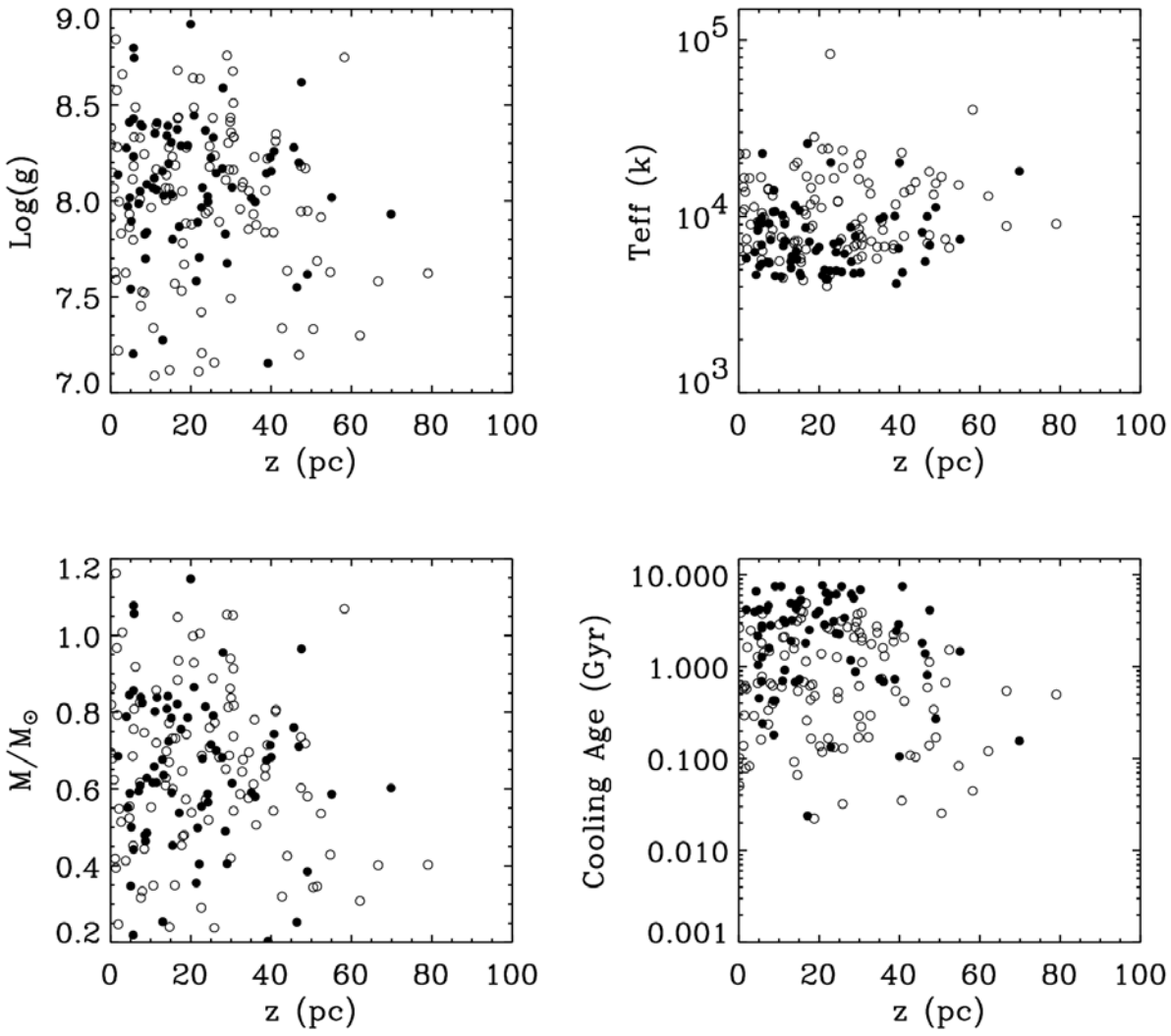

Figure 6: Physical parameters determined for the WDs with parallax distances using the model grid interpolation method described in Monteiro et al. (2005)
Source: The authors.

following equation for the time spent on the Main Sequence to obtain the total ages FBB01:

$$t_{MS} = 10 \cdot M^{-2.5}\ Gyr \quad (2)$$

in which M is the mass of the progenitor (in solar units), and t_{MS} is the main sequence lifetime in *Gyr*.

In Figure 9, we show the total age histograms for the various WD spectral types studied here (DA, DB, DC and DQ). Due to small number of objects, the DZ histogram was not constructed. For these histograms, we used the entire sample (including the WDs with distance estimates). It is important to point out that these distances were determined using a fixed $log(g)$= 8.0 and will, therefore, lead to uncertainties in cooling age and Main Sequence Lifetime, although this error should be small given the narrow distribution of $log(g)$ and masses of WDs as seen in Figure 7.

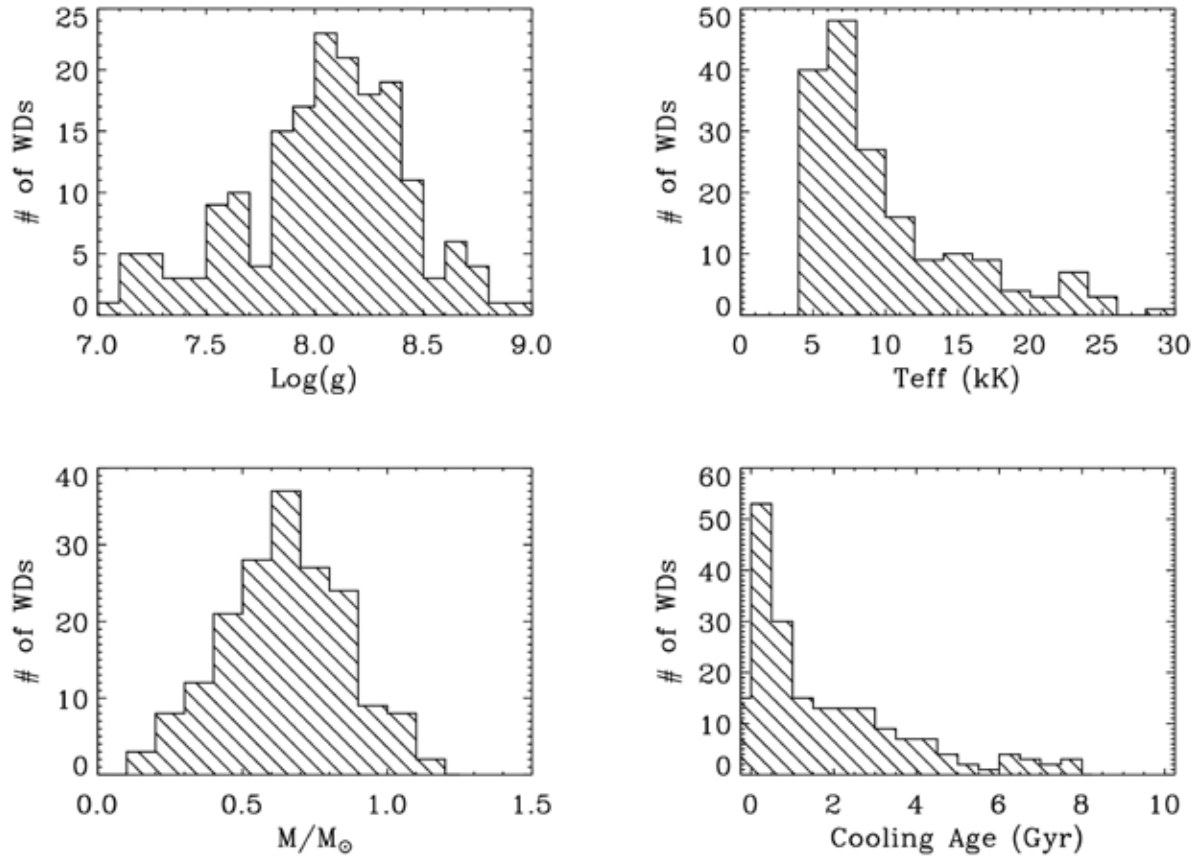

Figure 7: Histograms of physical properties of the WDs that have distances determined from parallax measurements
Source: The authors.

The histograms in Figure 9 show two distinct regions when the different spectral types are considered: before and after 5 Gyr. A factor ~4 decrease in the number of DA WDs older than about 5 Gyr is evident. The division is also present in the DB distribution, with no DBs being found older than about 5 Gyr. The DC distribution shows two clear peaks, one before and one after 5 Gyrs. The DQ distribution shows clear concentration of WDs younger than 5 Gyr, but no clear cut-off is found. That change is not entirely due to selection effects, i.e., decreased detection rate with larger distances because such an effect should present itself in a monotonically decreasing manner – not in a cutoff as in the DA, DB and DC histograms.

For the younger objects, we see that as the number of DAs decreases with total age, the number of DBs, DCs, and DQs increases, at least up until the 4Gyr peak present in those distributions. In Figure 10 we show the ratio of DB, DC and DQ to the number of DA as a function of total age. It is clear from this figure that the number of the non-DA WDs increases with increasing total age, reaching nearly a factor of 10 for DC WDs at about 10 Gyr.

The main cause for the behavior discussed previously is the evolution of the spectral types due to the cooling of the WDs, for example, the evolution to DCs from DBs caused by the lowering of the atmospheric temperature and reduction of

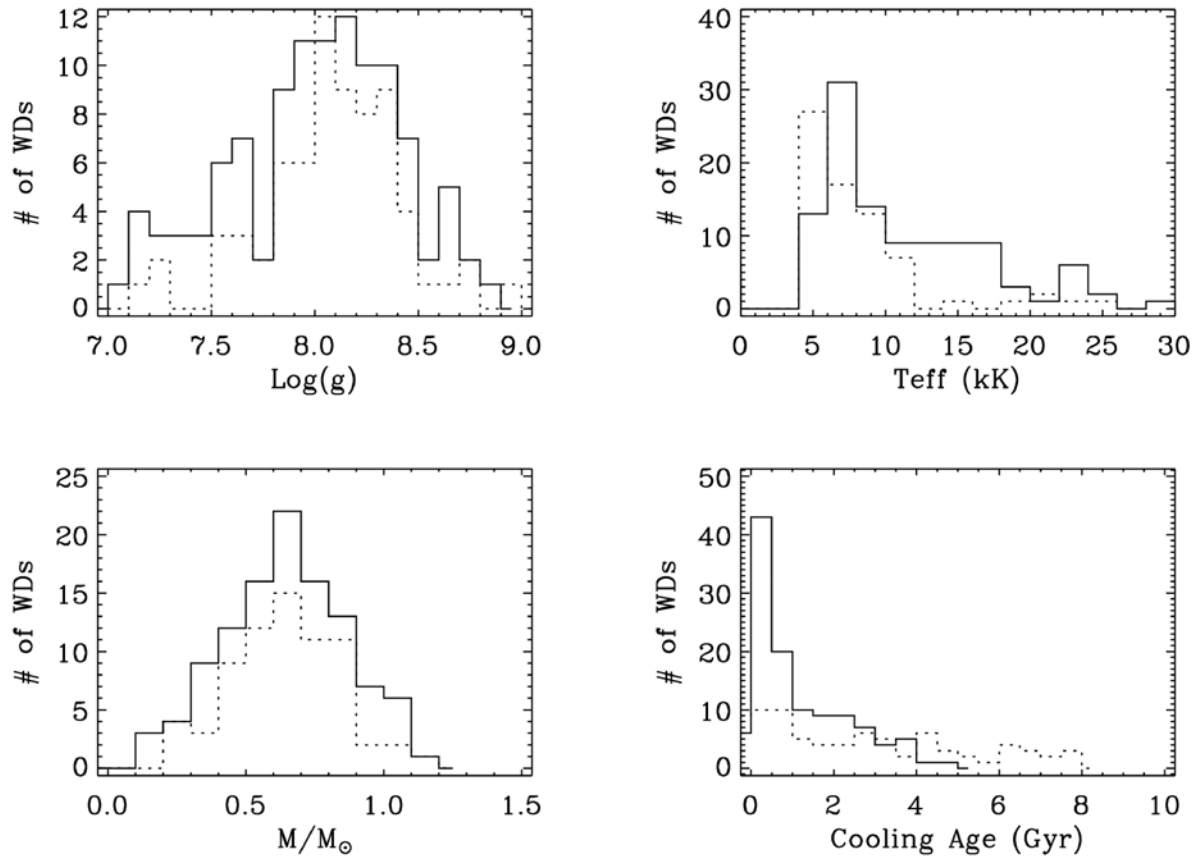

Figure 8: Histograms of physical properties of the WDs that have parallax distances, separated into DA (solid line) and non-DA (dotted line)
Source: The authors.

Helium line strengths [for detailed discussion see Kleinman et al. (2004)]. Other factors that could also affect this behavior are:

- cooling curve differences
- observational biases (proper motion and color selection effects)
- formation rates of DA and non-DAs and their evolution through time
- evolution from one spectral type to another (e.g. DA evolving to DC)

In Figure 11 we plot the cooling curves obtained from the Bergeron et al. (1995) models. Cooling curve differences between DA and non-DA are not important factors in the population differences over time because they only become significantly when different for cooling ages larger than 10 Gyr for WDs of $Log(g)$~8.0. In the extremes in which $Log(g)$~9.0, there are significant differences in the cooling curves for cooling ages as low as 5 Gyr, but the number of WDs in this $Log(g)$ range is quite small. The detection bias is also unlikely to be relevant in this population difference given that DAs are considerably more numerous in our local neighborhood and this is likely to be the case throughout the Galaxy (except perhaps in the Halo). Thus, it is hard to imagine a selection bias that yields about 5 times more DCs than DAs at 10 Gyr and only 10% at

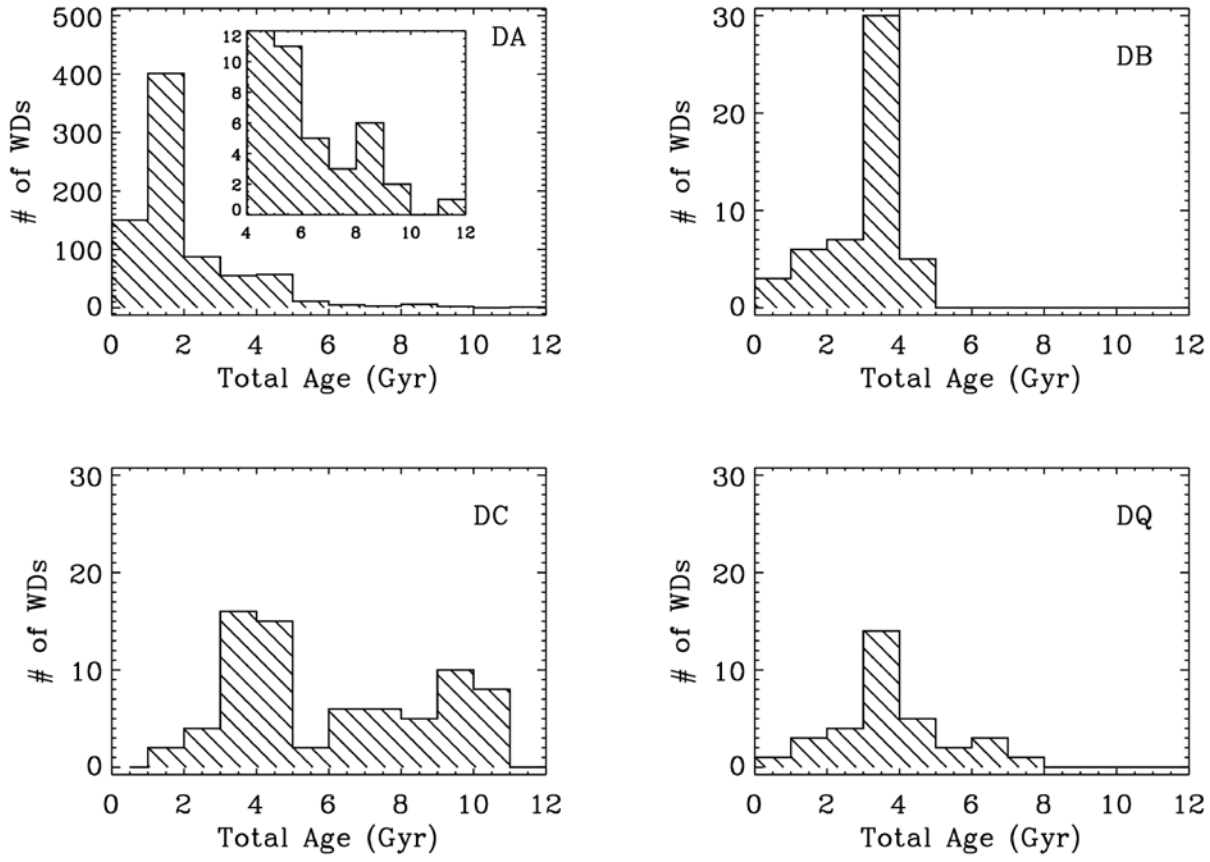

Figure 9: Histograms of WD total ages for the different spectral types studied. The bin size used was 1 Gyr

Source: The authors.

3 Gyr, especially considering that for a given age and $Log(g)$~8.0 there is very little difference in luminosity between both types. One could also argue that there is some uncertainty in the spectral types assigned to the stars given poor signal to noise spectra, but this is also unlikely to be relevant for the large factor observed at later ages. We are then left with the possibility of changing star formation properties as the Galaxy evolves and the possibility that there might be some evolution of the spectral types, with a portion of DAs evolving eventually to DCs. With this data set, it is impossible to separate between these two effects, or how important one is relative to the other with certainty.

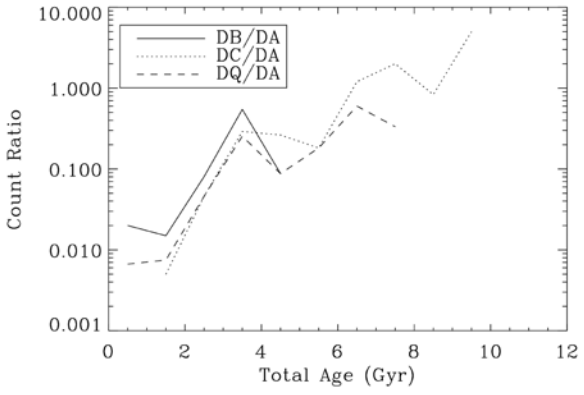

Figure 10: Ratio of the number counts of DB, DC and DQ relative to the DA counts as a function of total age. The bin size used was 1 Gyr

Source: The authors.

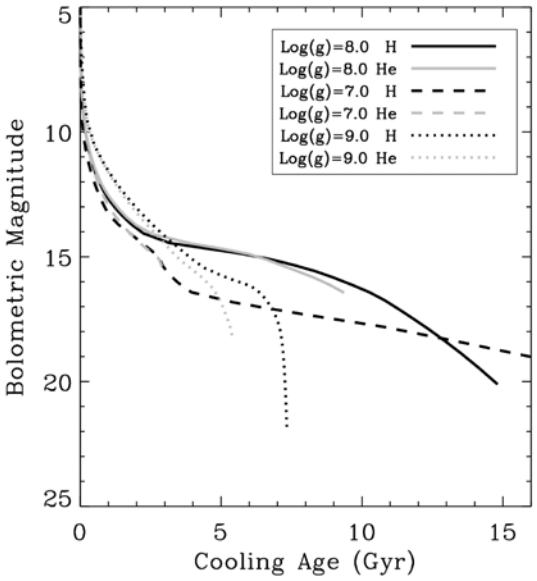

Figure 11: Cooling curves for H models (black lines) and He models (gray lines) for diferent *Log(g)* values
Source: The authors.

4 Luminosity function

The sample assembled in this work also provides us with an excellent data set to investigate the WD luminosity function. To construct luminosity functions, we use the method developed by Schmidt (1968). In this method, each star is assigned to a volume defined by the maximum distance at which the star can be detected, given sample limitations such as a magnitude limit. In our sample, we define the maximum distance at which any star can be detected as:

$$d_{max} = d \cdot 10^{\frac{Vlim - V}{5}} \quad (3)$$

in which V is the observed V magnitude, V_{lim} is the magnitude limit of the sample and d is the distance.

When constructing the luminosity function, the choice of the limiting magnitude is important. In Figure 12, we show the histogram of V magnitudes for our sample. The figure clearly shows that the sample no longer counts objects efficiently above V = 16.0, which we adopt as our magnitude limit. One must consider that our sample was drawn from a catalog comprised of many different surveys using various selection criteria, so our sample is the product of many different limiting magnitudes. Adopting a limiting magnitude of V= 16.0 means some stars in our sample had $d_{max} < d$, in which case we adopted $d_{max} = d$.

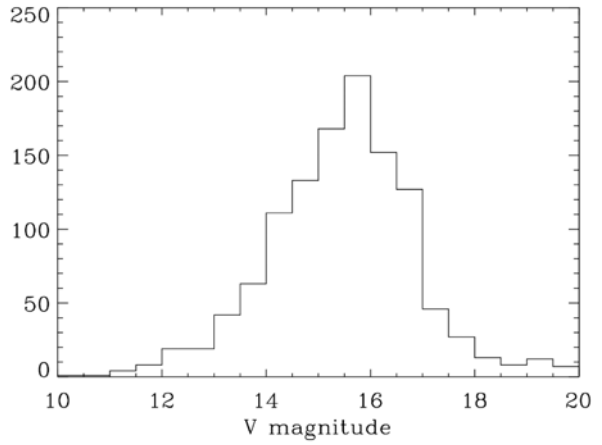

Figure 12: Histogram of V magnitudes for the full WD sample (parallax and model estimated distances) used in this work
Source: The authors.

Because the distances in our sample are comparable to the scale height of the disk [(obtained by Boyle (1989)], corrections for a non-uniform density of WDs should be applied. From d_{max}, we obtained V_{max} for each star by using the following expression from Tinney et al. (1993):

$$V_{max} = \Omega \left(\frac{h_0}{\sin b} \right)^3 [2 - (y^2 + 2y + 2)\, e^{-y}] \quad (4)$$

in which Ω is the solid angle covered by the sample, h_0 is the scale height and b is the Galactic latitude. For the value of Ω, we adopted 4π given the reasonably uniform coverage of the sky in our sample

(figure 2). We adopted the value of pc obtained by Boyle (1989) as the scale height, although we note that many authors have shown the weak dependence of the luminosity function on its value – see Wood (1992) for a complete discussion on the various dependencies of the luminosity function.

We calculated the luminosity function assuming that each star contributes to its particular luminosity or absolute magnitude bin. The error of each bin was determined following the prescription of Liebert et al. (1988):

$$\delta = \Sigma \frac{1}{V^2_{max}} \quad (5)$$

The luminosity function for the total sample studied in this work is presented in figure 13 as a function of absolute magnitude. In figure 14, we show the total luminosity function with absolute magnitudes converted to luminosities using the relation given in Liebert et al. (1988). The most important feature visible in the luminosity function is the turn-off at the faint end. In this region of the figure, two peaks were identified, one at and another at; however, due to the large error in the magnitude bin, we expect the latter to be not significant. Comparison of the turn-off to theoretical luminosity functions from other authors – for example, Wood (1992) shows that this is consistent with a disk age interval of 6 to 8 Gyr approximately. The peak at is consistent with the expected delay in cooling introduced by the onset of convective coupling and crystallization mentioned in Fontaine et al. (2001). According to Noh & Scalo (1990), it is possible that this peak could be partly due to a star formation burst and other pieces of evidence for such an event around 5 to 6 Gyr do exist [see Figure 8 of Noh & Scalo (1990)]. One minor peak is visible at and could also be related to a star burst event at 0.3 Gyr, as mentioned in Noh & Scalo (1990), and references therein.

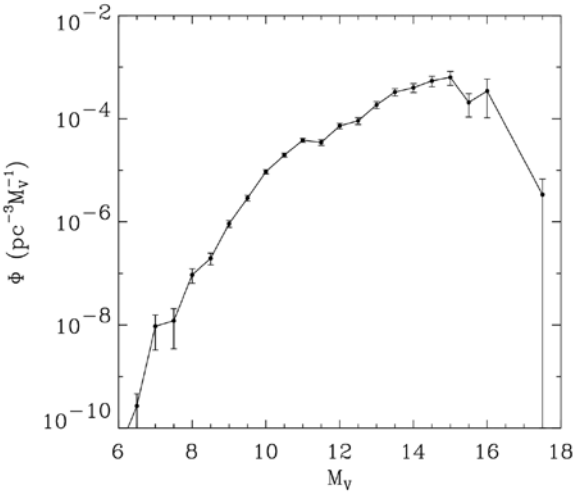

Figure 13: Luminosity function of the full WD sample (parallax and model estimated distances) studied in this work including all spectral types (0.5 mag bin size)
Source: The authors.

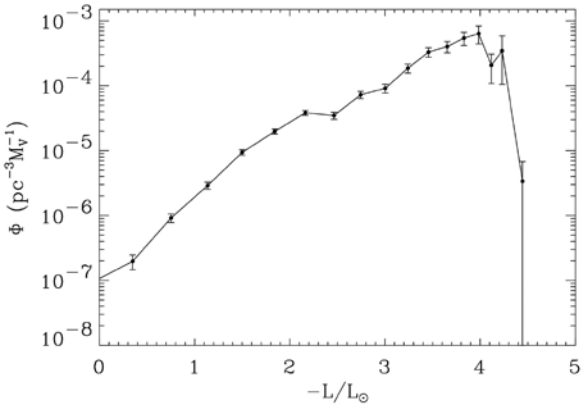

Figure 14: Luminosity function of the full WD sample (parallax and model estimated distances) studied in this work with absolute magnitudes converted to luminosities
Source: The authors.

The luminosity function for our sample is quite similar to the many efforts published previously – see Wood (1992), for example –, displaying the basic shape and structure. Some differences as to the actual density of WDs may appear and are likely due to our adoption of covering factor and scale height, which might not be the same in other efforts. The most important part however, the

turn-off at the faint end of the luminosity function, is in agreement with all other studies.

One important limitation in our construction of the luminosity function is that we derived it from a sample comprised of many surveys, with many different selection criteria. We, therefore, cannot apply the usual test to ascertain its completeness, meaning that the shape of the function should be correct, but actual density values will be incorrect. This should have no implication on the results discussed below, as our focus is not to determine actual spatial densities of WDs, but rather to try to identify particular events such as star formation bursts and structure relevant to the cooling theory.

To reveal differences among the various WD types, we also constructed luminosity functions for the different spectral types of WDs in our sample. In figure 15, we show the luminosity functions for each type as a function of . In figure 16, we break out each luminosity function and show error bars for each magnitude bin. There is remarkable structure in these luminosity functions. We re-identify the peak at approximately MV = 11.0 (–Log(L/L⊙) ≈ 2.3) in the DA and DB luminosity functions, as pointed out by Harris et al. (2006) and Noh & Scalo (1990). We also identify a clear concentration of DB WDs in a narrow magnitude range, between MV = 9.0 and MV = 13.0, indicating a very narrow age interval for this particular class of WDs.

The turn off at the faint end is even more interesting when the different types of WDs are considered. The sample of DBs, DQs, DAs and DCs shows a turn-off point at increasingly faint magnitude values respectively. DZs do not appear to turn off at any point. A secondary peak is also apparent in the DC luminosity function at M_V ~12:. We have investigated how robust these structural differences are by examining WDs within given distance constraints because

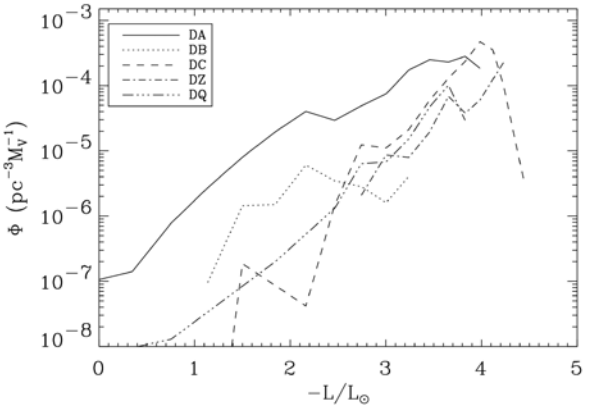

Figure 15: Luminosity functions of the subsample studied in this work with spectral types discriminated. The bin size used was 0.5 mag
Source: The authors.

for volume limited samples of small distances we are less affected by selection and detection biases. The luminosity functions presented here are consistent down to 25 pc albeit with smaller numbers.

5 Conclusions

We presented here a study of a sample of *Villanova Catalog of Spectroscopically Identified White Dwarfs* using model techniques to obtain their physical characteristics and Galactic distribution. For stars with reliable parallaxes we determined their full physical properties ($log(g)$, mass, cooling age). Examining the distribution of these properties with respect to the WD distances to the disk, we have not found any obvious relation. The histograms for the masses of the DA and non-DA WDs showed narrow distributions with peaks at approximately $log(g)$~8.1, in agreement with results found by other authors.

For the WDs that had (B-V) or (b-y) colors we have estimated distances, based on the assumption that $log(g)$=8.0 for all objects, and shown that they are relatively reliable (errors of about

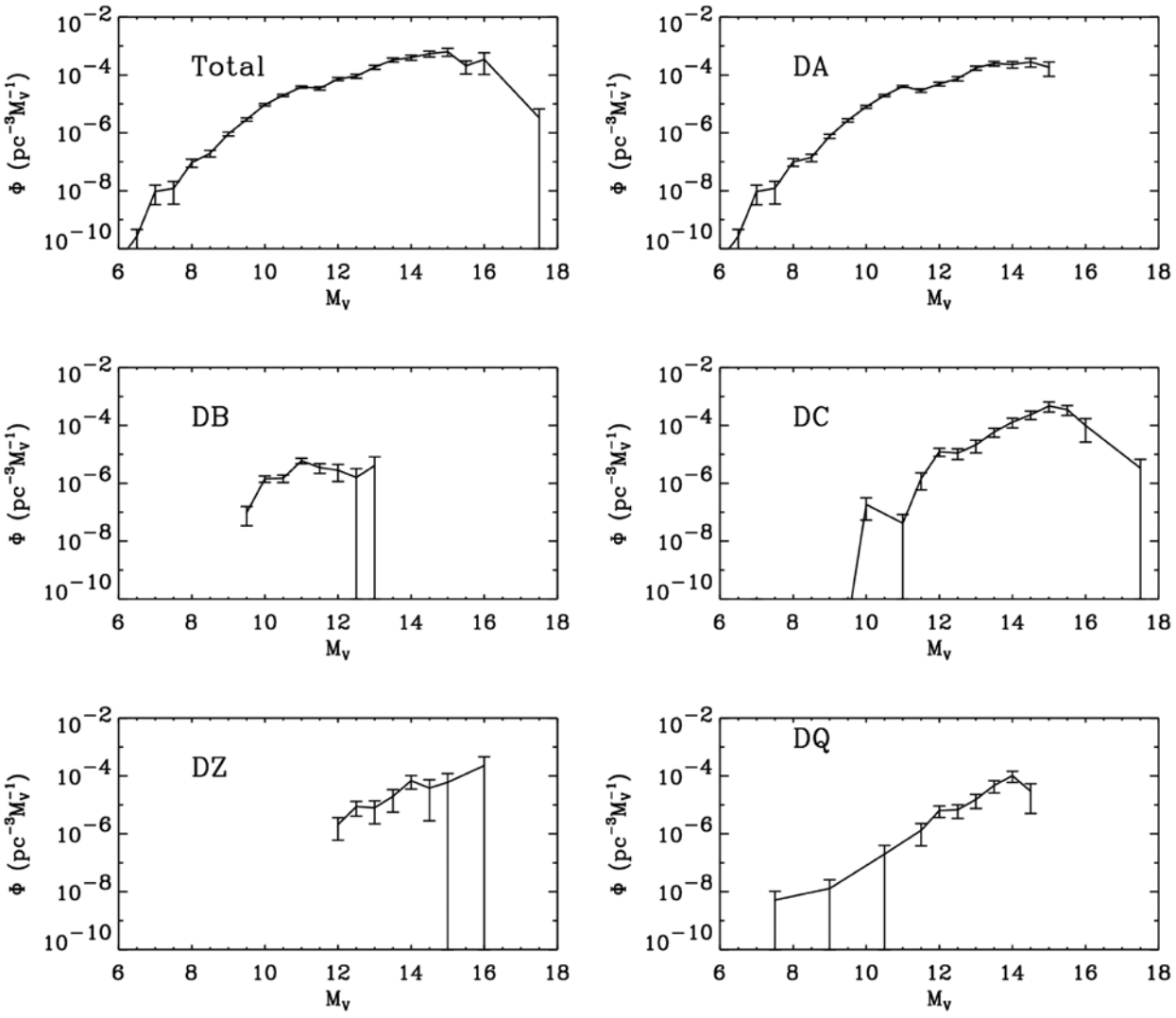

Figure 16: Luminosity functions of the sample studied in this work, including the error bars, for all spectral types. The bin size used was 0.5 mag

Source: The authors.

26% as discussed previously) given the minimal information required for their determination. With this sample of 1072 stars with parallax and estimated distances we have determined the solar distance to the Galactic disk and found that to be above the plane. This value is found to be in general agreement with other determinations given by Humphreys & Larsen (1995).

We have also inspected the binary fraction of the sample of WDs. In particular, we investigated the binary fraction and how it varied as a function of disk distance z. Our sample did not present any noticeable gradient in the binary fraction out to 100 pc. Even though our sample did not encompass a large volume, the lack of a gradient could indicate that there is no reduction of the concentration of binaries at larger distances to the disk and more complete samples to greater distances are crucial to further test this result.

Using the precise parallax distances as well as the model estimated distances, we have con-

structed the luminosity function for our sample as well as for each individual spectral type as specified in the original catalog. The luminosity function for the whole sample does not present any new feature, but corroborates many previous results. The few differences related to the actual density for a given magnitude bin are likely due to our adopted value for the scale height of the WD distribution relative to the Galactic disk, as well as different distance estimates. However, we have focused on the relative shape of the luminosity function for the whole sample as well as the luminosity functions for individual spectral types. We have shown that each individual type has its own characteristic shape, likely related to the star formation history and physical processes relevant to each one. The luminosity function for DA white dwarfs agrees well with all previous results and shows some structure likely related to previously identified star formation bursts and details of the cooling processes involved. The luminosity function for DB WDs showed a very localized distribution indicating that this particular spectral type is short lived. The other spectral types showed more or less similar slopes with distinct turn-off points. The DC WDs seem to be representative either of the last stage of evolution for WDs or a favored formation scenario for DCs in early times in the Galaxy, given that they represent a large fraction of the older WDs, in contrast with DAs, which clearly dominate on the younger side. However, precise theoretical studies, similar to the one performed by Wood (1992) now should focus on each individual spectral type and the relevant physical processes. With the advances in large survey projects and theoretical models for WDs this could prove to be a powerful tool to further our understanding of fundamental stellar and Galactic evolution.

References

BERGERON, P.; WESWMAEL, F.; BEAUCHAMP, A. Photometric Calibration of Hydrogen- and Helium-Rich White Dwarf Models. *PASP*, v. 107, p. 1047, 1995.

BERGERON, P.; LEGGETT, S. K.; RUIZ, M. T. Photometric and Spectroscopic Analysis of Cool White Dwarfs with Trigonometric Parallax Measurements. *Astrophysical Journal*, v. 133, p. 413, 2001.

BERGERON, P.; RUIZ, M. T.; HAMUY, M.; LEGGETT, S. K.; CURRIE, M. J.; LAJOIE, C. P.; DUFOUR, P. On the Interpretation of High-Velocity White Dwarfs as Members of the Galactic Halo. *Astrophysical Journal*, v. 625, p. 838.

BOYLE, B. J. The space distribution of DA white dwarfs. *Monthly Notices of the Royal Astronomical Society*, v. 240, p. 533, 1989.

DUFOUR, P.; BERGERON, P.; FONTAINE, G. Detailed Spectroscopic and Photometric Analysis of DQ White Dwarfs. *Astrophysical Journal*, v. 627, p. 404, 2005.

FONTAINE, G.; BRASSARD, P.; BERGERON, P. The Potential of White Dwarf Cosmochronology. \pasp, v. 113, p. 409, 2001.

GREEN, R. F. The luminosity function of hot white dwarfs. *Astrophysical Journal*, v. 238, p. 685, 1980.

GREEN, R. F.; SCHIMIDT, M.; LIEBERT, J. The Palomar-Green catalog of ultraviolet-excess stellar objects. *Astrophysical Journal*s, v. 61, p. 305, 1986.

GREENSTEIN, J. L. The degenerate stars with hydrogen atmospheres. I. *Astrophysical Journal*, v. 233, p. 239, 1979.

HARRIS, H. C., et al. Cool White Dwarfs in the Sloan Digital Sky Survey. *Astronomical Journal*, v. 131, p. 571, 2006.

HUMPHREYS, R. M.; LARSEN, J. A. The Sun's Distance Above the Galactic Plane. *Astronomical Journal*, v. 110, p. 2183, 1995.

IBEN, I. J.; LAUGHLIN, G. A study of the white dwarf luminosity function. *Astrophysical Journal*, v. 341, p. 312, 1989.

JOSHI, Y. C. Interstellar extinction towards open clusters and Galactic structure. \mnras, v. 362, p. 1259, 2005.

KLEINMAN, S. J. et al. A Catalog of Spectroscopically Identified White Dwarf Stars in the First Data Release of the Sloan Digital Sky Survey. *Astrophysical Journal*, v. 607, p. 426, 2004.

LIEBERT, J.; DAHN, C. C.; MONET, D. G. The luminosity function of white dwarfs. *Astrophysical Journal*, v. 332, p. 891, 1988.

LUYTEN, W. J. Intercomparison of spectroscopic and spectrophotometric methods. *Astronomical Journal*, v. 63, p. 194, 1958.

McCOOK, G. P.; SION, E. M. 1977, Villanova University Observatory Contributions, Villanova, Penn: Villanova Press, 1977.

McCOOK, G. P.; SION, E. M. A Catalog of Spectroscopically Identified White Dwarfs. *Astrophysical Journal*s, v. 121, p. 1, 1999.

McCOOK, G. P.; SION, E. M. 2003, VizieR Online Data Catalog, 3235, 0.

MONTEIRO, H.; JAO, W.; HENRY, T.; SUBASAVAGE, J.; BEAULIEU, T. Ages of White Dwarf-Red Subdwarf Systems *Astrophysical Journal*, v. 638, p. 446, 2006.

NOH, H. R.; SCALO, J. History of the Milky Way Star Formation Rate from the White Dwarf Luminosity Function. *Astrophysical Journal*, v. 352, p. 605, 1990.

OSWALT, T. D.; SMITH, J. A.; WOOD, M. A.; HINTZEN, P. A lower limit of 9.5 Gyr on the age of the Galactic disk from the oldest white dwarf stars. *Nature*, v. 382, p. 692, 1996.

SALARIS, M.; DOMINGUEZ, I.; GARCIA-BERRO, E.; HERNANZ, M.; ISERN, J.; MOCHKOVITCH, R. The Cooling of CO White Dwarfs: Influence of the Internal Chemical Distribution. *Astrophysical Journal*, v. 486, p. 413, 1997.

SILVESTRI, N. M.; OSWALT, T. D.; HAWLEY, S. L. Wide Binary Systems and the Nature of High-Velocity White Dwarfs. *Astronomical Journal*, v. 124, p. 1118, 2002.

SILVESTRI, N. M.; HAWLEY, S. L.; OSWALT, T. D. The Chromospheric Activity and Ages of M Dwarf Stars in Wide Binary Systems *Astronomical Journal*, v. 129, p. 2428, 2005.

SION, E. M.; LIEBERT, J. The space motions and luminosity function of white dwarf. *Astrophysical Journal*, v. 213, p. 468, 1977.

SION, E. M.; FRITZ, M. L.; McMULLIN, J. P.; LALLO, M. D. Kinematical tests of white dwarf formation channels and evolution. *Astronomical Journal*, v.96, p. 251, 1988.

SCHMIDT, M. Space Distribution and Luminosity Functions of Quasi-Stellar Radio Sources. *Astrophysical Journal*, v. 151, p. 393, 1968.

TINNEY, C. G.; REID, I. N.; MOULD, J. R. The faintest stars - From Schmidt plates to luminosity functions. *Astrophysical Journal*, v. 414, p. 254, 1993.

WEIDEMANN, V. Revision of the initial-to-final mass relation *Astronomy & Astrophysics*, v. 363, p. 647, 2000.

WOOD, M. A. Constraints on the age and evolution of the Galaxy from the white dwarf luminosity function. *Astrophysical Journal*, v.386, p.539, 1992.

WOOD, M. A.; OSWALT, T. D. White Dwarf Cosmochronometry. I. Monte Carlo Simulations of Proper-Motion- and Magnitude-limited Samples Using Schmidt's 1/Vmax Estimator. *Astrophysical Journal*, v. 497, p. 870, 1998.

Recebido em XX set. 2007 / aprovado em X out. 2007

Para referenciar este texto

MONTEIRO, H.; JAO, W.-C.; KANAAN, A. White-Dwarfs in the thin-disk: physical properties and luminosity functions. *Exacta*, São Paulo, v. 5, n. 2, p. 375-391, jul./dez. 2007.